

Meson B_c annihilation to leptons and inclusive light hadronsXing-Gang Wu,^{1,*} Chao-Hsi Chang,^{1,2,†} Yu-Qi Chen,^{1,2,‡} and Zheng-Yun Fang^{3,§}¹*Institute of Theoretical Physics, Chinese Academy of Sciences, P.O. Box 2735, Beijing 100080, China*²*CCAST (World Laboratory), P.O. Box 8730, Beijing 100080, China*³*Department of Physics, Chongqing University, Chongqing 400044, China*

(Received 12 September 2002; revised manuscript received 10 February 2003; published 5 May 2003)

The annihilation of the B_c meson to leptons and inclusive light hadrons is analyzed in the framework of nonrelativistic QCD (NRQCD) factorization. We find that the decay mode, which escapes from the helicity suppression, contributes a sizable fraction width. The branching ratio due to the contributions from the color-singlet component of the B_c meson can be of the order of 10^{-2} . The contributions from the color-octet components are estimated. With the consideration of the NRQCD velocity scaling rule, we find that the color-octet contributions are sizable too, especially in a certain phase space of the annihilation. They are greater than (or comparable to) those from the color-singlet component. A few observables on the spectrum of charged leptons (e, μ) relevant to the contributions are suggested that may be used as measurements of the evidence of the color-octet components in future B_c experiments. A kind of typical “long-distance contributions” in the annihilation is also estimated.

DOI: 10.1103/PhysRevD.67.094001

PACS number(s): 13.20.Jf, 12.38.Bx, 12.39.Hg

I. INTRODUCTION

The discovery of the B_c meson by the Collider Detector at Fermilab (CDF) Collaboration [1] is one of the important discoveries in heavy quark physics, and the Collaboration’s results are consistent with theoretical predictions [2–7] concerning theoretical uncertainties and experimental errors. More B_c events in the new runs of the Fermilab Tevatron than those of the discovery and much more events by several orders at the CERN Large Hadron Collider (LHC) are expected [2]. Therefore, a thorough experimental study of the B_c meson and more precise comparisons with theoretical predictions on its properties, especially, its various decay modes, will be available in the foreseeable future.

One of the most interesting decays is the pure leptonic decay, because the decay amplitude is proportional to the decay constant f_{B_c} and the Cabibbo-Kobayashi-Maskawa (CKM) matrix element V_{cb} . In principle, it can be used to measure f_{B_c} if we know the value of V_{cb} , or vice versa. However, the pure leptonic decay modes suffer from helicity suppression with small leptonic mass in the decay modes. The suppression is not severe for the $B_c \rightarrow \tau \nu_\tau$ decay mode only, where it is difficult to be detected because its resultant state contains at last two neutrinos.

There is no helicity suppression if more particles are included in the decay modes. Such an example is the radiative leptonic decay $B_c \rightarrow \gamma l^+ \nu_l$, which has been analyzed in Refs. [8–12]. Their results show that the decay branching ratios are of the order of 10^{-5} for $l = (\mu, e)$, which is much larger than that of the pure leptonic decay of the e mode and comparable to that of the μ mode. The relatively larger

branching ratio may make it possible to be measured at the LHC.

In this paper, we analyze new annihilation decay modes, i.e., the “semi-inclusive” decay $B_c \rightarrow l^+ \nu_l + \text{light hadrons}$, although the authors of Ref. [13] have considered the exclusive decay precisely with two pions. Here light hadrons are produced from the emitted soft or/and hard gluons, i.e., we are interested not in any specific light hadron(s) but in sum all of them. The annihilation modes escape from the effects of helicity suppression due to additional gluons being emitted in the final state. Since the annihilation involves a pair heavy quarks, we assume that it can be analyzed in the framework of the factorization of the effective theory, non-relativistic QCD (NRQCD) [14]. According to this framework, the decay width can be factored into a sum of products of short-distance coefficients and NRQCD long-distance matrix elements. The short-distance coefficients can be calculable perturbatively in a power series of α_s at the energy scale of the heavy quark mass. We may determine them by matching the results obtained by full QCD (calculated at the threshold) and those by NRQCD. Generally, the long-distance matrix elements can be estimated roughly by means of the velocity power counting rule of NRQCD. For convenience, throughout the paper we will call the contributions that may be taken into account by NRQCD factorization as “short-distance” contributions.

NRQCD considers a physical quarkonium, B_c , or \bar{B}_c state as an expansion of different Fock states, so the annihilation may occur via different Fock states. According to NRQCD, the annihilation modes $B_c \rightarrow l^+ \nu_l + \text{light hadrons}$ can be carried out via the leading-order Fock states $|c\bar{b}_1(^1S_0)\rangle$, $|c\bar{b}_8(^3S_1)g\rangle$, and $|c\bar{b}_8(^1P_1)g\rangle$ and higher-order Fock states as well. With a naive order estimate, the annihilation modes for the leading order may be the modes $(c\bar{b})_1(^1S_0) \rightarrow l^+ \nu_l + gg$, via the leading Fock state in velocity v and states an order higher in QCD, or those such as $(c\bar{b})_8(^3S_1) \rightarrow l^+ \nu_l$

*Email address: xgwu@itp.ac.cn

†Email address: zhangzx@itp.ac.cn

‡Email address: ychen@itp.ac.cn

§Email address: zfyang@cqu.edu.cn

+ g and $(c\bar{b})_8(^1P_1)\rightarrow l^+\nu_l+g$, etc., via higher-order Fock states but states an order lower in QCD because of the compensation in order for the Fock states and QCD couplings. Therefore, for the decay $B_c\rightarrow l^+\nu_l$ + light hadrons we need to consider several short-distance processes. Potentially the annihilation modes can be used to probe the contributions from the components of the different higher-order Fock states, and this is why we investigate annihilation modes quantitatively in this paper in the framework of NRQCD factorization. Namely, we estimate the decay rate accordingly by taking the potential model value for the color-singlet matrix element that relates to the wave function (derivative of the wave function) at the origin directly and by means of the consideration of velocity scaling rule of NRQCD for the color-octet matrix elements.

In the conventional potential model, heavy quark and $(c\bar{b}),(\bar{c}b)$ systems are just bound states of the heavy quark and antiquark in a color singlet [15]. Thus when the annihilation of the B_c meson is estimated by means of the potential model, only the factor of the long-distance matrix elements for the color-singlet component in NRQCD factorization formulas can be determined, i.e., only color-singlet matrix elements in NRQCD may be related to the wave functions of the potential model. The color-singlet and short-distance contributions may be estimated by means of matching the calculations for the coefficients and by means of the potential model for the long-distance matrix elements.

In Ref. [9], some typical ‘‘long-distance contributions’’ [we use quotation marks here because we mean the contributions from certain bound states as intermediate state(s) of the decay] to the leptonic radiative decays have been taken into account, and results show that such contributions are negligible in comparison with the short-distance contributions. In fact, in the annihilation modes discussed here, there are also similar ‘‘long-distance contributions.’’ Therefore in this paper we also estimate the ‘‘long-distance contributions.’’

The paper is organized as follows. In Sec. II, we briefly outline the formulas for annihilation modes within the NRQCD framework first, then in Sec. II A we present the method for calculating the short-distance coefficient for color-singlet one, which relates to the process $(c\bar{b})_1\rightarrow l^+\nu_l gg$. In Sec. II B we calculate the short-distance coefficients for color-octet ones, which relate to $(c\bar{b})_8\rightarrow l^+\nu_l g$ of higher-order Fock states (color-octet ones). In Sec. III, we estimate typical ‘‘long-distance contributions’’ of the color-singlet leptonic decays by using the so-called generalized instantaneous approximation [3,4]. In Sec. IV, we present the numerical results and discussions.

II. NRQCD FACTORIZATION ANALYSIS

In the nonrelativistic heavy quark limit, there are several distinct energy scales in heavy quark and antiquark bound state systems. The heavy quark masses m_c and m_b relate to the largest energy scale, while the off-shell three-momentum μv and the typical binding energy μv^2 are comparatively small, where $\mu=m_c m_b/(m_c+m_b)$ is the reduced mass of

the system and $v\sim O(\alpha_s)$ is the relative velocity between the heavy quark and the antiquark. NRQCD now is established by integrating out the energy scale effects at heavy quark mass μ . In the effective theory NRQCD, the heavy quark and antiquark are described by nonrelativistic two-component fields. A physical state of the B_c meson can be decomposed into a sum of a set of Fock states:

$$|B_c\rangle=O(v^0)|c\bar{b}_1(^1S_0)\rangle+O(v^1)|c\bar{b}_8(^1P_1)g\rangle+O(v^1)|c\bar{b}_8(^3S_1)g\rangle+\dots$$

According to the velocity scaling rule [14], the probability of each Fock state in the above expansion scales as a definite power of v . Namely, the leading Fock state of the B_c meson is $|c\bar{b}_1(^1S_0)\rangle$, whose probability is of order $O(v^0)$. The next leading Fock states are $|c\bar{b}_8(^1P_1)g\rangle$ and $|c\bar{b}_8(^3S_1)g\rangle$, whose probability is of order $O(v^2)$, etc. As notation throughout this paper, we denote the color of the $(c\bar{b})$ pair with a subscript (1 for color singlet and 8 for color octet), with the spin angular momentum quantum number being set in parentheses.

Because c and \bar{b} are heavy quarks, the annihilation of these quarks occurs at a short distance in the sense of the perturbative QCD (PQCD). The size of the B_c meson is of the order $O(1/(v\mu))$, where $\mu=m_b m_c/(m_b+m_c)$ is the reduced mass of the \bar{b} quark, which is distinctly separated from the annihilation. Thus NRQCD factorization formulas can also be used to analyze decays of the B_c meson. Hence we adopt the formalism of NRQCD for the calculations in this paper. According to NRQCD factorization formulas, the decay width can be factored into

$$\Gamma=\frac{1}{2M}\sum_n C_n\langle B_c|\hat{O}_n|B_c\rangle, \quad (1)$$

where $C_n(n=1,2,\dots)$ are the short-distance coefficients and $\langle B_c|\hat{O}_n|B_c\rangle(n=1,2,\dots)$ are NRQCD ‘‘long-distance’’ matrix elements. The short distance coefficients, being expanded in powers of α_s , can be calculated by PQCD. In contrast, the long-distance matrix elements are the ‘‘average’’ values of the operators $\hat{O}_n, n=1,2,\dots$ (local, gauge invariant, and relevant to the annihilation modes), which in the NRQCD framework consist of nonrelativistic four-quark operators, and measure the inclusive probability of finding a pair of $c\bar{b}$ with suitable color and angular momentum etc. By the velocity scaling rule the possibilities in the B_c meson are given in orders of v . The $(\bar{b}c)$ pair of the B_c meson may be not only in color-singlet Fock states but also in color-octet states, and all of them may annihilate at short distance with proper gluon(s). The matrix elements correspond to relevant color-singlet Fock states or color-octet states accordingly. The lowest-order decay process in v for the color-singlet state is $(\bar{b}c)_1\rightarrow l\nu_l+gg$, while those for the color-octet states are $(\bar{b}c)_8(^1P_1)\rightarrow l\nu_l+g$ and $(\bar{b}c)_8(^3S_1)\rightarrow l\nu_l+g$.

Hence up to the relevant order, the factorization for the decay width reads as the follows:

$$\begin{aligned} \Gamma = & \frac{1}{2M} \left[C_1(^1S_0) \frac{1}{M^2} \langle B_c | \psi_c^\dagger \chi_b \chi_b^\dagger \psi_c | B_c \rangle \right. \\ & + C_8(^3S_1) \frac{1}{M^2} \langle B_c | \psi_c^\dagger \sigma^i T^a \chi_b \chi_b^\dagger \sigma^i T^a \psi_c | B_c \rangle \\ & + C_8(^1P_1) \frac{1}{M^4} \langle B_c | \psi_c^\dagger \left(-i \frac{1 \leftrightarrow}{2} D \right) T^a \chi_b \chi_b^\dagger \\ & \left. \times \left(-i \frac{1 \leftrightarrow}{2} D \right) T^a \psi_c | B_c \right], \end{aligned} \quad (2)$$

where $C_1(^1S_0)$, $C_8(^3S_1)$, and $C_8(^1P_1)$ are short-distance coefficients of order $G_F \alpha_s^2$, $G_F \alpha_s$, and $G_F \alpha_s$ (the lowest order in weak and strong interactions), respectively. The matrix elements of the three terms in square brackets scales as v^3 , v^5 , and v^5 , comparatively. Note that here we have adopted the normalization for the meson states as $\langle B_c(\mathbf{P}') | B_c(\mathbf{P}) \rangle = 2E_P (2\pi)^3 \delta^3(\mathbf{P}' - \mathbf{P})$. Since we focus on annihilation modes only, where in addition to the leptons, light hadrons must also be included, so the contributions from pure leptonic annihilation modes to the coefficient $C_1(^1S_0)$ appearing in Eq. (2) should be eliminated.

Now let us compute these short-distance coefficients. Namely, to obtain the coefficients, we calculate the modes with PQCD precisely, and then match the results with those from the NRQCD factorized formulas precisely. The amplitude for the decay $B_c(P) \rightarrow l^+(k_4) + \nu_l(k_5) + X$ can generally be written as

$$M = \frac{G_F V_{cb}}{\sqrt{2}} \langle l \nu_l | j^\mu | 0 \rangle \langle X | J_\mu^w | B_c \rangle, \quad (3)$$

where V_{cb} is the CKM matrix element, and j^μ and J_μ^w are the weak currents for $l \nu$ leptons and $c \bar{b}$ quarks, respectively.

Then the decay width can be expressed as

$$\Gamma = \frac{G_F^2 V_{cb}^2}{4M (2\pi)^6} \int \frac{d^3 \vec{k}_4}{2\varepsilon_4} \frac{d^3 \vec{k}_5}{2\varepsilon_5} L^{\mu\nu}(k_4, k_5) \cdot t_{\mu\nu}(P, k_4 + k_5), \quad (4)$$

where

$$L^{\mu\nu}(k_4, k_5) = \bar{u}(k_5) \gamma^\mu (1 - \gamma_5) v(k_4) \bar{v}(k_4) \gamma^\nu (1 - \gamma_5) u(k_5), \quad (5)$$

$$t_{\mu\nu}(P, k) = \text{Im} \int d^4 x e^{ikx} \langle B_c(P) | J_\mu^w(x) J_\nu^w(0) | B_c(P) \rangle,$$

are the leptonic tensor and the hadronic tensor, respectively. The $c \bar{b}$ quark currents in the hadronic tensor precisely are $J_\mu^w = \bar{\psi}_c \gamma_\mu (1 - \gamma_5) \psi_b$ and $J_\nu^w = \bar{\psi}_b \gamma_\nu (1 - \gamma_5) \psi_c$. The leptonic tensor $L^{\mu\nu}$ can easily be calculated and reads:

$$L^{\mu\nu} = 8[k_4^\mu k_5^\nu + k_5^\mu k_4^\nu - g^{\mu\nu} (k_4 \cdot k_5) - i \varepsilon^{\mu\nu\alpha\beta} k_{4\alpha} k_{5\beta}], \quad (6)$$

where $\varepsilon^{\mu\nu\alpha\beta}$ is the total antisymmetric tensor.

According to the factorization, the hadronic tensor contains both short-distance coefficients and long-distance matrix elements. Based on NRQCD, the hadronic tensor can be factored as

$$\begin{aligned} t^{\mu\nu}(P, k) \equiv & \text{Im} \int d^4 x e^{ikx} \langle B_c(P) | J^{\mu w}(x) J^{\nu w}(0) | B_c(P) \rangle \\ = & \left[d_1^{\mu\nu}(^1S_0; P, k) \frac{1}{M^2} \langle B_c | \psi_c^\dagger \chi_b \chi_b^\dagger \psi_c | B_c \rangle \right. \\ & + d_8^{\mu\nu}(^3S_1; P, k) \frac{1}{M^2} \langle B_c | \psi_c^\dagger \sigma^i T^a \chi_b \chi_b^\dagger \sigma^i T^a \psi_c | B_c \rangle \\ & + d_8^{\mu\nu}(^1P_1; P, k) \frac{1}{M^4} \langle B_c | \psi_c^\dagger \left(-i \frac{1 \leftrightarrow}{2} D \right) \\ & \left. \times T^a \chi_b \chi_b^\dagger \left(-i \frac{1 \leftrightarrow}{2} D \right) T^a \psi_c | B_c \right]. \end{aligned} \quad (7)$$

Here $d_1^{\mu\nu}(^1S_0; P, k)$, $d_8^{\mu\nu}(^3S_1; P, k)$, and $d_8^{\mu\nu}(^1P_1; P, k)$ are the factors of the short-distance coefficients that we need to compute precisely. Comparing Eq. (4) with Eq. (2), they are related to the coefficients $C_1(^1S_0)$, $C_8(^3S_1)$, and $C_8(^1P_1)$ in Eq. (2) precisely as follows:

$$C_1(^1S_0) = \frac{G_F^2 V_{cb}^2}{2(2\pi)^6} \int \frac{d^3 \vec{k}_4}{2\varepsilon_4} \frac{d^3 \vec{k}_5}{2\varepsilon_5} L_{\mu\nu}(k_4, k_5) \cdot d_1^{\mu\nu}(^1S_0; P, k), \quad (8)$$

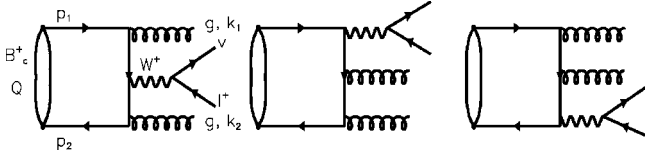
$$C_8(^3S_1) = \frac{G_F^2 V_{cb}^2}{2(2\pi)^6} \int \frac{d^3 \vec{k}_4}{2\varepsilon_4} \frac{d^3 \vec{k}_5}{2\varepsilon_5} L_{\mu\nu}(k_4, k_5) \cdot d_8^{\mu\nu}(^3S_1; P, k), \quad (9)$$

$$C_8(^1P_1) = \frac{G_F^2 V_{cb}^2}{2(2\pi)^6} \int \frac{d^3 \vec{k}_4}{2\varepsilon_4} \frac{d^3 \vec{k}_5}{2\varepsilon_5} L_{\mu\nu}(k_4, k_5) \cdot d_8^{\mu\nu}(^1P_1; P, k), \quad (10)$$

with $k = k_4 + k_5$.

These coefficients can be evaluated by using the threshold expansion method [16]. In this method, the on-shell ($c \bar{b}$) pair near threshold with specified quantum number is annihilated. The amplitudes for the processes at the quark level are calculated in PQCD and expanded according to the relative velocity v in the framework of factorization formulas. In addition, the real processes of the B_c annihilation may be calculated in the framework of NRQCD and ‘‘suffer’’ a factorization. By matching these two calculation methods, the short-distance coefficients can be ‘‘read off.’’

More precisely the coefficients $C_1(^1S_0)$ and $d_1^{\mu\nu}(^1S_0; P, k)$ are determined by matching the process $(c \bar{b})_1(^1S_0) \rightarrow l^+ \nu_l + gg$, while $C_8(^3S_1)$ and $d_8^{\mu\nu}(^3S_1; P, k)$,

FIG. 1. Three Feynman diagrams for the decay $B_c \rightarrow l^+ \nu g g$.

$C_8(^1P_1)$, and $d_8^{\mu\nu}(^1P_1; P, k)$ are determined by matching the processes $(\bar{b}c)_8(^3S_1) \rightarrow l^+ \nu_l + g$; $(\bar{b}c)_8(^1P_1) \rightarrow l^+ \nu_l + g$ with the calculations on the annihilation modes of the B_c meson in terms of NRQCD, respectively. In the following two sections, we show how to determine these coefficients by matching relevant modes precisely.

A. Short-distance coefficient for the color-singlet component

In this section, we use the threshold expansion method to determine the short-distance coefficients $C_1(^1S_0)$ and $d_1^{\mu\nu}(^1S_0; P, k)$ by matching the process $c(p_1)\bar{b}(p_2) \rightarrow l^+(k_4)\nu_l(k_5) + g(k_1)g(k_2)$, where $(c\bar{b})$ is in a color-singlet Fock state. At the lowest order, there are only six Feynman diagrams contributing to the amplitude. Three diagrams correspond to those in Fig. 1 and the other three can be obtained by exchanging the gluons. The amplitude is given by

$$M = \frac{G_F V_{cb}}{\sqrt{2}} \langle l \nu_l | j_\mu | 0 \rangle A^\mu, \quad (11)$$

where A^μ is defined by

$$A_\mu \equiv \langle g g | J_\mu^w | (\bar{b}c)_1(^1S_0) \rangle = \sum_{i=1,2,\dots,6} A_{\mu,i}. \quad (12)$$

The six terms in the amplitude correspond to the six Feynman diagrams.

The three terms that are shown in Fig. 1, are given by

$$A_{\mu,1} = \frac{g_s^2 \delta^{ab}}{2\sqrt{3}} \bar{b}(p_2) \epsilon^b(k_2) \frac{1}{\not{k}_2 - \not{p}_2 - m_b} \times \gamma_\mu (1 - \gamma_5) \frac{1}{\not{p}_1 - \not{k}_1 - m_c} \epsilon^a(k_1) c(p_1), \quad (13)$$

$$A_{\mu,2} = \frac{g_s^2 \delta^{ab}}{2\sqrt{3}} \bar{b}(p_2) \epsilon^a(k_1) \frac{1}{\not{p}_2 - \not{k}_1 - m_b} \epsilon^b(k_2) \times \frac{1}{\not{p}_1 - \not{k} + m_b} \gamma_\mu (1 - \gamma_5) c(p_1), \quad (14)$$

$$A_{\mu,3} = \frac{g_s^2 \delta^{ab}}{2\sqrt{3}} \bar{b}(p_2) \gamma_\mu (1 - \gamma_5) \frac{1}{\not{p}_2 - \not{k} + m_c} \times \epsilon^b(k_2) \frac{1}{\not{p}_1 - \not{k}_1 - m_c} \epsilon^a(k_1) c(p_1), \quad (15)$$

where $\bar{b}(p_2)$ and $c(p_1)$ are the Dirac four-component spinors of the antiquark \bar{b} and the quark c , respectively. $\epsilon^a(k_1)$ and $\epsilon^b(k_2)$ are the polarization vectors of the two gluons with color indices a, b respectively. The other three terms of the amplitude can be obtained by exchanging the gluon vertices.

The momenta of \bar{b} and c quarks are related to their total and relative momenta P and q as follows:

$$p_1 = \mu_c P + q, \quad p_2 = \mu_b P - q \quad (16)$$

here $\mu_c \equiv m_c / (m_c + m_b)$ and $\mu_b \equiv m_b / (m_c + m_b)$. In the case of the lowest-order calculation for the S wave, which is what we consider, the relative momentum q can be approximately set to null, i.e., $q=0$; hence the momenta can be further simplified as

$$p_1 = \mu_c P, \quad p_2 = \mu_b P.$$

Then the hadronic tensor $t^{\mu\nu}(P, k)$ for the annihilation mode $[(c\bar{b})_1(^1S_0)] \rightarrow l^+ + \nu_l + g + g$ can be expressed as

$$t^{\mu\nu}(P, k) = \frac{1}{(2\pi)^2} \int \frac{d^3\vec{k}_1}{2\varepsilon_1} \frac{d^3\vec{k}_2}{2\varepsilon_2} A^{\mu*} A^\nu \delta^4(P - k - k_1 - k_2) = d_1^{\mu\nu}(^1S_0; P, k) \frac{1}{M^2} \langle (c\bar{b})_1(^1S_0) | \psi_c^\dagger \chi_b \chi_b^\dagger \psi_c | \times (c\bar{b})_1(^1S_0) \rangle + \dots, \quad (17)$$

where \dots denotes terms, that correspond to pure leptonic decays and to the $(c\bar{b})$ pair with other quantum numbers we are not interested in here.

The integration over the gluon phase space can be evaluated. The details of the calculations are given in the Appendix, but we outline the basic steps here. By introducing three Lorentz invariant variables $z = (k_1 + k_2)^2 / M^2$, $y = k^2 / M^2$, and $x_l = 2k_4 \cdot P / M^2$, the hadronic tensor $t^{\mu\nu}(P, k)$ can be expressed in terms of these variables. The short-distance coefficients $d_1^{\mu\nu}(^1S_0; P, k)$ can then be obtained by matching Eq. (17) and Eq. (7).

The most general form of the tensor $d_1^{\mu\nu}(^1S_0; P, k)$ can be expressed as

$$d_1^{\mu\nu}(^1S_0; P, k) = A g^{\mu\nu} + B P^\mu P^\nu + C P^\mu k^\nu + D k^\mu P^\nu + E k^\mu k^\nu. \quad (18)$$

However, when we contract it with the leptonic tensor, Eq. (5), the contributions from the last three terms of Eq. (18) vanish due to the fact that we ignore the lepton masses totally, and, as a result, the leptonic weak current (even includ-

ing the axial component) is conserved. Thus only the first two terms are effective. The detailed calculations and expressions of the coefficients A and B can be found in the Appendix.

Since we are interested in the energy spectrum of the charged leptons (e, μ), which is measurable, we also give the coefficients before integrating over the leptonic energy x_l , and those before integrating over z , y , and x_l :

$$C_1(^1S_0) = \frac{G_F^2 V_{cb}^2 M^4}{2^9 \pi^4} \int dy dz dx_l [d_1^{\mu\nu}(^1S_0; P, k) L_{\mu\nu}] \times \vartheta(x_l) \vartheta(1+y-z-x_l) \vartheta(Y), \quad (19)$$

where the new variable

$$Y \equiv \frac{(1+y-z-x_l)^2 x_l^2}{4} - \left(y - \frac{(1+y-z-x_l)x_l}{2} \right)^2$$

is introduced. By setting $Y=0$ and drawing the Dalitz diagram for the process, we may determine the integration area for y , z , and E_l (or x_l). The result for the integration area may also be found in the Appendix. Since the integrations are quite complicated so we carries out them numerically.

If one carries out the integrations in the order of first integrating y and z and, then x_l , then, before doing the last integration for x_l , the measurable energy spectra of the charged leptons $d\Gamma/dx_l$ can be obtained. Thus we evaluate the integrations in this order and discuss the obtained energy spectra in Sec. IV.

In order to check the numerical results, we also use a different order of integrations. Namely, we try to integrate over the variable of the leptons y last, but integrate over the other variables of the leptons and those of gluons first. In this way, we need to change the lepton tensor from $L^{\mu\nu}$ to $N^{\mu\nu}$:

$$N^{\mu\nu} \equiv \frac{4\pi}{3} (k^\mu k^\nu - k^2 g^{\mu\nu}). \quad (20)$$

To complete the phase space integrations in this order, and having all the other variables of the phase space integrated out, we reach the step at which only three independent integration variables: y , ε_s (the sum of the gluons' energies), and ε_d (the difference of the gluons' energies) need to be integrated out. Then to carry out the integrations further, we need to determine the integration area for these three variables by using Dalitz diagrams. The determined integration area is $0 \leq y \leq 1$, $-\varepsilon_d^{\max} \leq \varepsilon_d \leq \varepsilon_d^{\max}$, and $-\varepsilon_s^{\min} \leq \varepsilon_s \leq \varepsilon_s^{\max}$, where

$$\begin{aligned} \varepsilon_d^{\max} &= \sqrt{(M - \varepsilon_s)^2 - M^2 y}, \\ \varepsilon_s^{\max} &= M(1 - \sqrt{y}), \\ \varepsilon_s^{\min} &= \frac{M(1-y)}{2}. \end{aligned} \quad (21)$$

Thus the coefficient $C_1(^1S_0)$ is written as

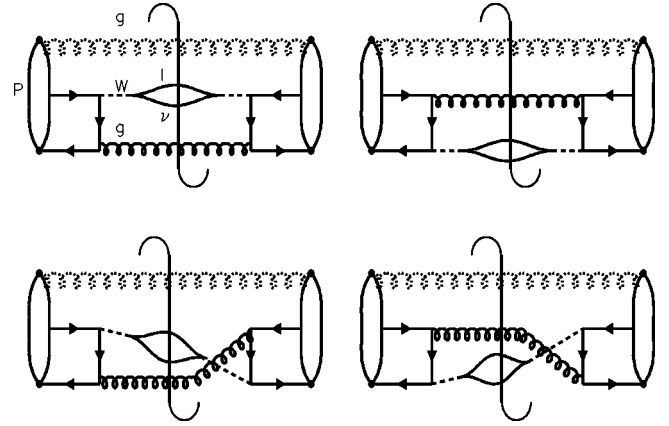


FIG. 2. The diagrams for the width of the annihilation modes $B_c \rightarrow l^+ \nu g$, where B_c is indicated in two possible color-octet Fock states. The vertical line cut in the diagrams is understood as the imaginary part being taken.

$$C_1(^1S_0) = \int dy \int_{\varepsilon_s^{\min}}^{\varepsilon_s^{\max}} \int_{-\varepsilon_d^{\max}}^{\varepsilon_d^{\max}} f_l(\varepsilon_s, \varepsilon_d, y) d\varepsilon_s d\varepsilon_d, \quad (22)$$

where the integrand $f_l(\varepsilon_s, \varepsilon_d, y)$ is obtained straightforwardly in the order of the integrations as described. Since the result for each step is very tedious, we do not present the procedure here. We have done the computations carefully and indeed find that the final results for the annihilation rate obtained by the numerical integrations in the two orders are the same, so we have a good check on the numerical result. In fact, as a semifinished result in this integration order, the ‘‘spectrum’’ $d\Gamma/\Gamma_{B_c} dy$ on $y = k^2/M^2$ may be obtained too, but it is not easy to measure experimentally so we do not present the curves of the spectrum here.

B. Short-distance coefficients for the color-octet components

In this section, we use the threshold expansion method to determine the short-distance coefficients $C_8(^3S_1)$, $d_8^{\mu\nu}(^3S_1; P, k)$, and $C_8(^1P_1)$, $d_8^{\mu\nu}(^1P_1; P, k)$ by matching the modes $c(p_1)\bar{b}(p_2) \rightarrow l^+(k_4)\nu_l(k_5) + g(k_1)$, where $c\bar{b}$ are color-octet states but obviously with different spin angle momentum. At the lowest order, there are only two Feynman diagrams contributing to the amplitude of the decay modes. The width can be dictated by the imaginary part of four of the forward amplitude diagrams as indicated by the Feynman diagrams in Fig. 2. The amplitude accordingly is given by

$$M^{a'} = \frac{G_F V_{cb}}{\sqrt{2}} \langle l \nu_l | j^\mu | 0 \rangle A_\mu^{a'}, \quad (23)$$

where $A_\mu^{a'}$ is defined by

$$A_\mu^{a'} \equiv \langle g | J_\mu^{w'} | (\bar{b}c)_8 \rangle = \sum_{i=1,2} A_{\mu,i}^{a'}, \quad (24)$$

where $a = 1, \dots, 8$ are the color indices. The amplitudes, corresponding to the Feynman diagrams in Fig. 2, are given by

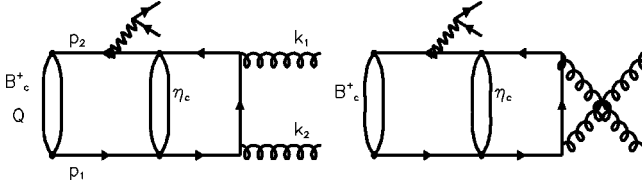


FIG. 3. The diagrams for long-distance effects.

$$A_{\mu,1}^{a'} = \frac{1}{2} \text{Tr}[T^a T^b] g_s \bar{b}(p_2) \times \gamma_\mu (1 - \gamma_5) \frac{1}{\not{p}_1 - \not{k}_1 - m_c} \not{\epsilon}^b(k_1) c(p_1), \quad (25)$$

$$A_{\mu,2}^{a'} = \frac{1}{2} \text{Tr}[T^a T^b] g_s \bar{b}(p_2) \not{\epsilon}^b(k_1) \times \frac{1}{\not{p}_2 - \not{k}_1 - m_b} \gamma_\mu (1 - \gamma_5) c(p_1). \quad (26)$$

In the cases of the S -wave and P -wave $c\bar{c}$ pair that we are considering and to the lowest-order approximation, we expand the expression in powers of q , the relative momentum, and keep terms only up to linear ones of q (because we are performing the leading-order calculations only).

Then the hadronic tensor $t^{\mu\nu}(P, k)$ for the annihilation mode $(c\bar{c})_1(^1S_0) \rightarrow l^+ \nu_l g$ can be expressed as

$$\begin{aligned} t^{\mu\nu}(P, k) &= \int \frac{d^3 \vec{k}_1}{2\varepsilon_1} A^{a'\mu*} A^{a'\nu} \delta^4(P - k - k_1) \\ &= d_8^{\mu\nu}({}^3S_1; P, k) \frac{1}{M^2} \langle (c\bar{b})_8^3 S_1 | \psi_c^\dagger \sigma^i T^a \chi_b \chi_b^\dagger \sigma^i \\ &\quad \times T^a \psi_c | (c\bar{b})_8^3 S_1 \rangle + d_8^{\mu\nu}({}^1P_1; P, k) \\ &\quad \times \frac{1}{M^4} \langle (c\bar{b})_8^1 P_1 | \psi_c^\dagger (-i \frac{1}{2} \overleftrightarrow{D}) \\ &\quad \times T^a \chi_b \chi_b^\dagger (-i \frac{1}{2} \overleftrightarrow{D}) T^a \psi_c | (c\bar{b})_8^1 P_1 \rangle + \dots, \quad (27) \end{aligned}$$

where \dots denotes the terms corresponding to the $c\bar{c}$ pair being in the other states, which we are not interested in here.

The integration over the gluon phase space can be performed easily. Thus with suitable projection for spin angular momentum, Eq. (9) and Eq. (10), the short-distance coefficients can be computed easily:

$$C_8({}^3S_1) = \int dx_l \frac{\alpha_s M^6 (m_b^2 + m_c^2) G_F^2 V_{bc}^2}{24\pi^2 m_b^2 m_c^2} \times x_l [x_l - 4(1-x_l) \log(1-x_l)] \quad (28)$$

for the component $(c\bar{b})_8({}^3S_1)$, and

$$\begin{aligned} C_8({}^1P_1) &= \int dx_l \frac{\alpha_s M^6 G_F^2 V_{bc}^2}{12\pi^2 m_b^4 m_c^4 (1-x_l)} \{ x_l [M^2 \{ -3m_b m_c^3 (x_l - 1) + m_b^4 (x_l - 1)^2 + m_c^4 (x_l - 1)^2 - m_b^3 m_c (x_l - 1) (8x_l - 7) \\ &\quad + 2m_b^2 m_c^2 [3 + 2(x_l - 2)x_l] \} + 2M m_b m_c \{ -m_c^3 (x_l - 1) (2x_l - 7) + m_b m_c^2 (x_l - 1) (1 + 2x_l) + m_b^3 [(7 - 2x_l)x_l - 5] \\ &\quad + m_b^2 m_c [1 + x_l (6x_l - 11)] \} + 2m_b^2 m_c^2 \{ m_b^2 [11 + (x_l - 6)x_l] + m_c^2 [(x_l - 2)x_l - 1] + 2m_b m_c (x_l^2 - 3) \} \\ &\quad - (1 - x_l) \ln(1 - x_l) [M^2 \{ m_b^3 m_c (7 - 6x_l) + m_b^4 (x_l - 1) + m_c^4 (x_l - 1) + 2m_b^2 m_c^2 (2x_l - 3) + m_b m_c^3 (2x_l - 3) \} \\ &\quad - 2M m_b m_c \{ 5m_b^3 (x_l - 1) + m_b m_c^2 (x_l - 1) + m_b^2 m_c (1 - 7x_l) + m_c^3 (5x_l - 7) \} + 2m_b^2 m_c^2 \{ m_c^2 (x_l + 1) \\ &\quad - 2m_b m_c (x_l - 3) + m_b^2 (5x_l - 11) \}] \} \quad (29) \end{aligned}$$

for the component $(c\bar{b})_8({}^1P_1)$.

III. THE LONG-DISTANCE EFFECTS

Besides those between the b and \bar{c} quark pair in the initial state, there are also multi-soft-gluon interactions between the c and \bar{c} pair, which, as an intermediate state of the relevant decay (the \bar{b} quark has decayed into \bar{c} but the pair of c, \bar{c} has not annihilated yet), may make two quarks become a bound state. Since the interactions arise from multi-soft-gluon exchange, people generally attribute them to long-distance effects. In this section, we consider this kind of effect in the annihilation for the color-singlet component $B_c \rightarrow l^+ \nu_l g g$. Generally, with interactions the $c\bar{c}$ quark pair can form various bound states, such as $\eta_c, \eta_c', \dots, J/\psi, \psi', \dots$ (S -wave state), χ_c, \dots (P -wave states), etc. Since η_c is the ground state and has the proper quantum number, it contributes to the decay with the greatest amount among the bound states, so we take η_c as a typical state to estimate long-distance effects. The multi-soft-gluon interactions between the c and \bar{c} pair in color-octet components cannot form a bound state (color confinement) so the effects cannot be very great and we do not discuss them here.

By taking into account a possible intermediate meson state η_c as a typical state to consider the long-distance effects in Fig. 3 (there is only η_c as the intermediate state), the amplitude is

$$\begin{aligned}
M = & -\frac{G_F V_{cb} g_s^2}{2\sqrt{6}} (2\pi)^4 \delta(P-Q-k) \bar{u}_\nu(k_5) \gamma^\mu (1 \\
& - \gamma_5) v_{\bar{l}}(k_4) \sum_{\vec{Q}=k_1+\vec{k}_2} \frac{\delta_{ab} \epsilon_m^a(k_1) \epsilon_n^b(k_2)}{2Q_0(Q_0-\omega_{\vec{Q}}+i\epsilon)} i \int \frac{d^4 r}{(2\pi)^4} \left(\text{Tr} \left[\chi_{Q(r)} \gamma_m \frac{1}{\frac{1}{2}Q+t-k_2-m_c} \gamma_n \right] \right. \\
& \left. + \text{Tr} \left[\chi_{Q(r)} \gamma_n \frac{1}{\frac{1}{2}Q+t-k_1-m_c} \gamma_m \right] \right) \int \frac{d^4 q}{(2\pi)^4} \text{Tr}[\chi_P(q) \Gamma_\mu \bar{\chi}_Q(q') (\mu_c \not{P} + \not{q} + m_c)], \quad (30)
\end{aligned}$$

where $\Gamma_\mu = \gamma_\mu(1 - \gamma_5)$, $\epsilon_m^a(k_1)$, and $\epsilon_n^b(k_2)$ are the polarization vectors of the two real gluons, $q = \mu_b p_1 - \mu_c p_2$ is the relative momentum between the two constitute quarks of the B_c meson, and $q' = q + \frac{1}{2}[(\mu_c - \mu_b)P + k]$, $r = 1/2(p_1 - p_2 + k)$ are those of the bound state η_c . Note that the equations

$$P = p_1 + p_2, \quad p_1 = \mu_c P + q, \quad p_2 = \mu_b P - q,$$

$$k = k_4 + k_5, \quad Q = k_1 + k_2$$

have been used in Eq. (30). $\omega_{\vec{Q}} \equiv \sqrt{\vec{Q}^2 + (M')^2}$ (M' is the mass of η_c). Usually off the mass shell, we have $Q_0 \neq \omega_{\vec{Q}}$ for the time component, but in the present case, the charged lepton energy may be $E_l \leq [M^2 - (M')^2]/2M$, so η_c , as an intermediate bound state, may reach its mass shell, that is, $Q_0 = \omega_{\vec{Q}}$, and leads to a singularity in Eq. (30). This difficulty is due to the fact that we ignore the width of η_c . Thus here the width of η_c should be considered, i.e., replace $i\epsilon$ with $i(M'/Q_0)(\Gamma_{\eta_c})/2$ in the relevant propagator, where Γ_{η_c} is the total width of the bound state η_c of $c\bar{c}$. Then under the nonrelativistic approximation, we have

$$\begin{aligned}
\frac{1}{2Q_0(Q_0 - \omega_{\vec{Q}} + i\epsilon)} & \rightarrow \frac{1}{2Q_0[Q_0 - \omega_{\vec{Q}} + i(M'/Q_0)(\Gamma_{\eta_c}/2)]} \\
& \Rightarrow \frac{1}{Q^2 - (M')^2 + iM'\Gamma_{\eta_c}}.
\end{aligned}$$

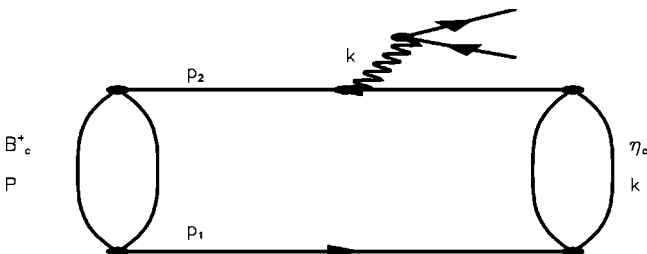


FIG. 4. Current matrix element for the long-distance effects.

Since only one intermediate bound state η_c is taken into account in Eq. (30), only the weak current matrix element corresponding to Fig. 3

$$\begin{aligned}
\langle \eta_c(Q) | \Gamma_\mu | B_c(P) \rangle = & i \int \frac{d^4 q}{(2\pi)^4} \text{Tr}[\chi_P(q) \\
& \times \Gamma_\mu \bar{\chi}_Q(q') (\not{p}_1 + m_c)] \quad (31)
\end{aligned}$$

and the amplitude for η_c annihilation

$$\begin{aligned}
\langle gg | \eta_c \rangle = & -\frac{g_s^2 \delta_{ab} \epsilon_m^a(k_1) \epsilon_n^b(k_2)}{2\sqrt{3}} \int \frac{d^4 r}{(2\pi)^4} \\
& \times \left(\text{Tr} \left[\chi_{Q(r)} \gamma_m \frac{1}{\not{p}_1 - \not{k}_2 - m_c} \gamma_n \right] \right. \\
& \left. + \text{Tr} \left[\chi_{Q(r)} \gamma_n \frac{1}{\not{p}_1 - \not{k}_1 - m_c} \gamma_m \right] \right) \quad (32)
\end{aligned}$$

are needed to be computed precisely. In fact, to compute the annihilation amplitude [Eq. (32)] is straightforward. However, to compute the weak current matrix element [Eq. (31)], which corresponds to the Feynman diagram in Fig. 4 (since $m_{B_c} \gg m_{\eta_c}$), one should pay more attention to the recoil effects for the intermediate process $B_c \rightarrow \eta_c$. We adopt the approach, the so-called generalized instantaneous approximation, which was proposed first in Ref. [3], to deal with the recoil effects. The details of the approximation may be found in Refs. [3,4,9], so here we will not repeat them but give the final result directly.

The weak current $\langle \eta_c(Q) | \Gamma_\mu | B_c(P) \rangle$ can be expressed by form factors f_+ , f_- :

$$\langle \eta_c(Q) | \Gamma_\mu | B_c(P) \rangle = f_+(P_\mu + Q_\mu) + f_-(P_\mu - Q_\mu). \quad (33)$$

Let us denote M and M' the masses of the two mesons B_c and η_c , respectively, and q_P and q_{PT} the two Lorentz covariant variables of the relative momentum q as follows:

$$q_P = \frac{P \cdot q}{M}, \quad q_{PT} = \sqrt{q_{PT}^2 - q^2},$$

and

$$\omega_i = \sqrt{m_i^2 + q_{PT}^2}, \quad \omega'_i = \sqrt{m_i'^2 + q'^2_{QT}}.$$

Then in terms of the generalized instantaneous approximation, the form factors f_{\pm} may be obtained as follows:

$$f_{\pm} = \pm \xi \left(\frac{\omega'_1 + \omega'_2}{M' m_c} \right),$$

where the factor, function ξ , is an overlapping integration of the wave functions $\phi'^*_Q(q'_{QT})$ and $\phi_P(|\vec{q}|)$ of the initial and final states in the c.m. system (c.m.s.) of the initial meson ($\vec{P} = \vec{0}$):

$$\xi = \left[\frac{2\omega'_2 m_b^2 m_c^2}{(p_1 \cdot p'_1 + m_b m_c) \omega_1 \omega'_1} \right]^{1/2} \times \int \frac{d^3 \vec{q}}{(2\pi)^3} \phi'^*_Q(q'_{QT}) \cdot \phi_P(|\vec{q}|). \quad (34)$$

Then long-distance effects due to η_c as an intermediate state may be estimated in terms of Eq. (30) straightforwardly.

Here we are interested in the decay channels $l = e, \mu$, so $m_l = 0$ and the contributions from the form factor f_- may be ignored. The differential decay rate due to the intermediate state η_c , $B_c \rightarrow \bar{l} \nu + \eta_c$, $\eta_c \rightarrow gg$ (the long-distance effects), finally can be written as follows:

$$\frac{d^3 \Gamma}{dx dy dz} = \frac{G_F^2 V_{cb}^2 M^5 \alpha_s^2 |\psi_{\eta_c}(0)|^2 f_+^2}{6M' \pi^4 [(M^2 z - M'^2)^2 + M'^2 \Gamma_{\eta_c}^2]} \times [(1-x)(x-y) - xz]. \quad (35)$$

Hence we have reached the right place to start the numerical calculations.

IV. NUMERICAL RESULTS AND DISCUSSIONS

First, we note that for numerical calculations, the parameters are taken as in Refs. [3,1,14,15]: $\alpha_s = 0.24$, $\Gamma_{B_c} = 2.714 \text{ ps}^{-1}$, $\psi(0) = 0.350 \text{ GeV}^{3/2}$, $\psi'(0) = 0.250 \text{ GeV}^{5/2}$. For comparison, we also quote the branching ratios of the pure leptonic decay for the B_c meson

$$\text{BR}(B_c \rightarrow e \nu_e) = 1.89 \times 10^{-9},$$

$$\text{BR}(B_c \rightarrow \mu \nu_\mu) = 7.57 \times 10^{-5},$$

$$\text{BR}(B_c \rightarrow \tau \nu_\tau) = 1.95 \times 10^{-2}.$$

Furthermore, to obtain more reliable values, we select the value of the quark masses with care. According to the discussions in Ref. [7], we take the effective masses of c and b quarks to be $m_c^{\text{eff}} = 1.5 \text{ GeV}$ and $m_b^{\text{eff}} = 4.9 \text{ GeV}$. For the mass of the B_c meson, we take pole masses of the quarks $m_c^{\text{pole}} = 1.88 \text{ GeV}$, $m_b^{\text{pole}} = 5.02$ [7,17–20] first, and then being consistent with that of potential model, the value of B_c mass $M = 6.352 \text{ GeV}$ is taken.

For the short-distance contributions of the process $B_c \rightarrow gg l \nu$, we find that when $E_l \leq (m_b^2 - m_c^2)/2m_b$, where E_l is the energy of the charged lepton, which is very different from that of the one photon radiative correction [9], the \bar{c} quark from the decay of \bar{b} quark may reach the mass shell. Thus to obtain a meaningful result, here we should also keep the “width” of c quark in its propagator, namely, we should make the following replacement:

$$\frac{q + m_c}{q^2 - m_c^2 + i\epsilon} \rightarrow \frac{q + m_c}{q^2 - m_c^2 + i(4m_c \Gamma_c)},$$

where Γ_c is the total width of an on-shell c quark, and from D decays its value should be $\Gamma_c \approx 1.229 \text{ ps}^{-1}$ [6].

For the annihilation modes of the color-singlet component, $B_c \rightarrow gg l \nu$, since the color-singlet matrix element $\langle B_c | \psi_c^\dagger \chi_b \chi_b^\dagger \psi_c | B_c \rangle$ may be related to the wave function at origin squared $|\psi(0)|^2$ and if only short-distance contributions are taken into account, the branching ratio may be computed precisely:

$$\begin{aligned} \text{BR}^{\text{short}}(B_c \rightarrow l \nu_l gg) &= \frac{\Gamma(B_c \rightarrow l \nu_l gg)}{\Gamma_{B_c}} \\ &= 2.71 \times 10^{-2} \quad (l = e, \mu). \end{aligned} \quad (36)$$

If only the long-distance contributions are taken into account (as in Sec. III), the branching ratio may be computed too:

$$\begin{aligned} \text{BR}^{\text{long}}(B_c \rightarrow l \nu_l gg) &= \frac{\Gamma(B_c \rightarrow l \nu_l \eta_c \rightarrow l \nu_l gg)}{\Gamma_{B_c}} \\ &= 4.45 \times 10^{-3} \quad (l = e, \mu). \end{aligned} \quad (37)$$

In fact, as the theoretical estimate on the “total branching” ratio of the annihilation mode $B_c \rightarrow gg l \nu$ for the color singlet component, these two kinds of contributions should be combined and the interference of these contributions should be considered too. To estimate the branching ratio for the color-singlet component, we should combine the amplitudes for the short-distance and long-distance contributions, but not the branching ratios, Eqs. (36) and (37). Then we obtain the final result

$$\text{BR}(B_c \rightarrow l \nu_l gg) = 3.62 \times 10^{-2} \quad (l = e, \mu). \quad (38)$$

From the above results [Eqs. (38), (36), and (37)] one may see that not only the pure long-distance contributions are quite big, which is different from the case for the radiative leptonic decays of the B_c meson, but also the interference of the short-distance and the long-distance contributions is not ignorable. To see the fact clearly, in addition to the branching ratios, we plot the energy spectrum for the short-distance contributions alone, both for the long-distance contributions alone and the total in Fig. 5. From the figure one may see that the short-distance contributions are dominant over the long-distance ones in the region close to the end of the spectrum. Therefore without special emphasis, the color-singlet component is always taken to mean the full short-distance contributions, and long-distance contributions are taken into account later on.

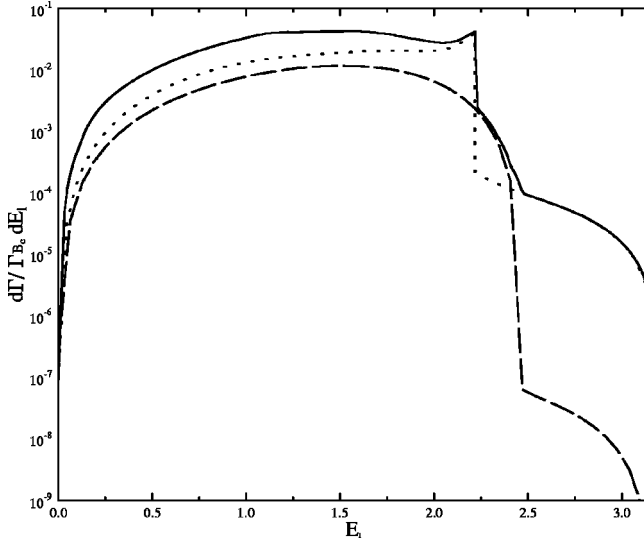


FIG. 5. The energy spectrum of the charged lepton for the annihilation $B_c \rightarrow l\nu g g$ ($l=e, \mu$). The solid line denotes the total color-singlet contributions. The dotted line denotes the pure short-distance contributions and the dashed line that for the pure long-distance contributions with η_c as an intermediate state.

For the annihilation modes of color-octet components, $B_c \rightarrow l\nu g$, up to now there is no reliable way to calculate the color-octet matrix elements $\langle B_c | \psi_c^\dagger \sigma^i T^a \chi_b \chi_b^\dagger \sigma^i T^a \psi_c | B_c \rangle$ and $\langle B_c | \psi_c^\dagger (-i\frac{1}{2}\overleftrightarrow{D}) T^a \chi_b \chi_b^\dagger (-i\frac{1}{2}\overleftrightarrow{D}) T^a \psi_c | B_c \rangle$ that are necessary for computing the annihilation.

In order to have a rough estimate of order, we, based on the velocity scaling rules of NRQCD [14], try to compare results with those of the S wave and those of the P -wave for the color-singlet components that can be related to the wave functions of the potential model. We assume

$$\langle B_c | \psi_c^\dagger \sigma^i T^a \chi_b \chi_b^\dagger \sigma^i T^a \psi_c | B_c \rangle \approx \Delta_S^2 \langle B_c | \psi_c^\dagger \sigma^i \chi_b \chi_b^\dagger \sigma^i \psi_c | B_c \rangle$$

and

$$\begin{aligned} & \langle B_c | \psi_c^\dagger (-i\frac{1}{2}\overleftrightarrow{D}) T^a \chi_b \chi_b^\dagger (-i\frac{1}{2}\overleftrightarrow{D}) T^a \psi_c | B_c \rangle \\ & \approx \Delta_P^2 \langle B_c | \psi_c^\dagger (-i\frac{1}{2}\overleftrightarrow{D}) \chi_b \chi_b^\dagger (-i\frac{1}{2}\overleftrightarrow{D}) \psi_c | B_c \rangle \end{aligned}$$

with Δ_S and Δ_P being $O(v)$ constants. Thus we may evaluate the color-octet contributions accordingly. In order to explore the characteristics of the color-octet components in the decays for the B_c meson, especially, to have comparisons with those of the color singlet, we try two possible choices for Δ_S and Δ_P : $\Delta_S \approx \Delta_P \approx 0.1$ for case (A) and $\Delta_S \approx \Delta_P \approx 0.3$ for case (B). The quantities Δ_S and Δ_P (for short Δ), in fact, measure how much Fock states with $(c\bar{b})$ are in octet configurations and are suppressed in comparison with the color-singlet state $(c\bar{b})$. Based on the consideration of the velocity scaling rule, the possible choices should be $\Delta \sim v$. Furthermore, since the reduced mass for the two-body systems plays a key role, and the reduced mass μ of B_c is closer to charmonium than bottomonium, here Δ should be closer

to that of charmonium than that of bottomonium. In fact, although according to Ref. [14], $v \sim 0.55$ for charmonium and $v \sim 0.3$ for bottomonium, here for a conserved choice of the B_c octet components, we still take a small $\Delta \sim 0.3$ case (B) instead. Because the theoretical velocity scaling rule should be tested by experiments, especially, for $(c\bar{b})$ and $(\bar{c}b)$, there is no experimental indication at all; thus in this paper we essentially focus on exploring the possibility with limited capacity in detecting the color-octet components experimentally, regardless of the correctness of the scale rule. To reach the “edge” of the experimental capacity, we also try to compute the annihilation with a much smaller color-octet component $\Delta \sim 0.1$ [case (A)]. The range of the values from case (A) to case (B) is well conserved from the velocity scaling rule, and, it may be conserved enough to obtain some idea of the possibility for a practical experimental capacity whether the color-octet components of the B_c meson can be detectable. Recently, the authors of Ref. [21], in terms of a fresh framework PNRQCD try to estimate the inclusive decays of charmonium, which is related to computing the long-distance matrix elements. We feel that experimental evidence, if available, provides good guidance for a fresh attempt.

The branching ratio of the color-octet modes is

$$\begin{aligned} \text{Br}(B_c(c\bar{b}_8(^3S_1)) \rightarrow l\nu_l g) &= 1.73 \times 10^{-4}, \\ \text{Br}(B_c(c\bar{b}_8(^1P_1)) \rightarrow l\nu_l g) &= 2.24 \times 10^{-5} \end{aligned} \quad (39)$$

for case (A) and

$$\begin{aligned} \text{Br}(B_c(c\bar{b}_8(^3S_1)) \rightarrow l\nu_l g) &= 1.55 \times 10^{-3}, \\ \text{Br}(B_c(c\bar{b}_8(^1P_1)) \rightarrow l\nu_l g) &= 2.02 \times 10^{-4} \end{aligned} \quad (40)$$

for case (B).

From the color-singlet and color-octet results above, we see that the helicity suppression of B_c in the studied annihilation modes is released. In total, the color-singlet to light-hadron mode is bigger than those of the color octet in cases (A) and (B).

Furthermore, since there is one or more gluon bremsstrahlung than the relevant pure leptonic decay modes, there is more freedom in the energy momentum and quantum number due to the gluon(s), such that the intermediate, \bar{c} quark, even a relevant bound state such as η_c , etc. (compounded by the produced \bar{c} quark and the “original” c quark in the B_c meson) may reach the mass shell. Thus the width of the studied annihilation modes may be as great as that of the semileptonic decay modes $b \rightarrow c l \nu$ or $B_c \rightarrow \eta_c l \nu$ correspondingly.

In Fig. 6, we plot the lepton energy spectrum of the annihilation modes for the leptons and light hadrons. From Fig. 6, it is interesting to point out that since the Fock space states for color octets are suppressed, in most regions of the phase space the annihilation modes due to the color octets (one-gluon bremsstrahlung) are smaller than that due to the color-singlet component (two-gluon bremsstrahlung), whereas the former may become greater in a certain region (with a high

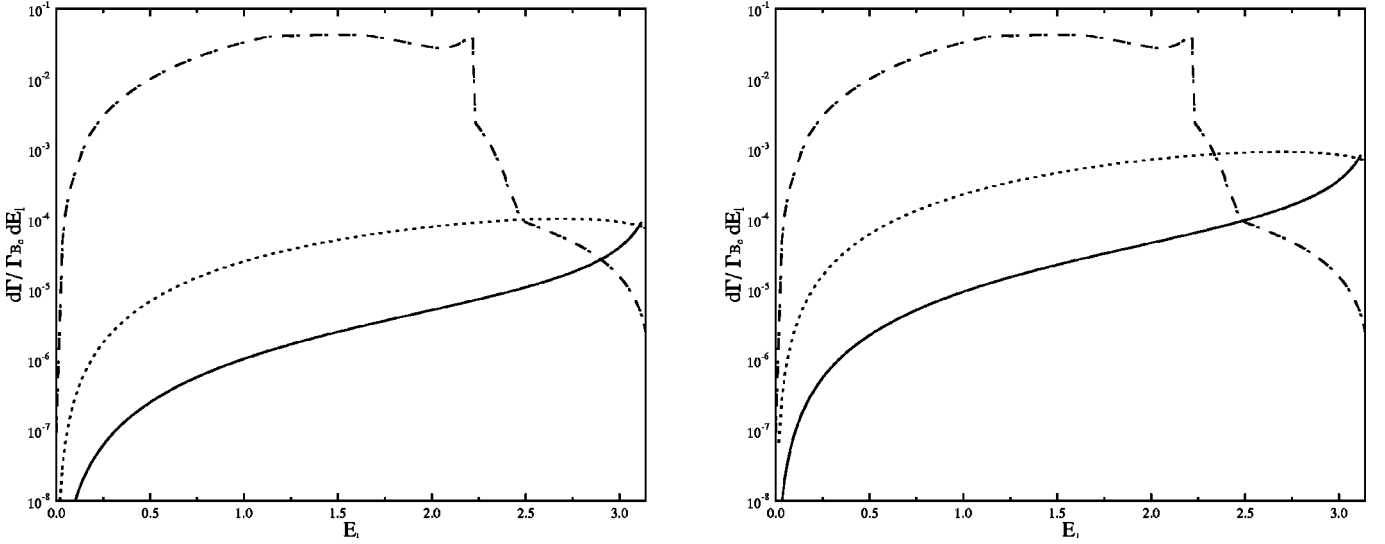


FIG. 6. The energy spectra of the charged lepton with different color-octet matrix elements for color-octet components versus that for color-singlet components. The left figure (a) is of those for case (A): $\Delta_S=0.1$ and $\Delta_P=0.1$. The right figure (b) is that for case (B): $\Delta_S=0.3$ and $\Delta_P=0.3$. The dashed line in the figures stands that for the color-singlet modes $B_c \rightarrow l^+ \nu l g$, ($l=e, \mu$). The dotted and the solid lines for the color-octet annihilation modes $B_c \rightarrow l^+ \nu g$ with $c\bar{b}_8(^3S_1)$ and $c\bar{b}_8(^1P_1)$, respectively.

momentum of the charged lepton) of the spectrum than that of the latter. Thus it is possible to see the color-octet contributions experimentally through studying the charged lepton energy spectrum of the inclusive decay $B_c \rightarrow l^+ \nu_l \dots$ carefully, especially around the end point of the spectrum.

In order to focus on the difference quantitatively in the spectrum of the charged leptons near the end point, where the color-octet contributions may become dominant over those of the color-singlet contributions, we introduce the ratios of the integrated partial decay widths of the B_c meson for the color-singlet and the color-octet modes,

$$R_S = \frac{\Gamma(c\bar{b}_1(^1S_0), x_l^{\text{cut}})}{\Gamma(c\bar{b}_1(^1S_0), x_l^{\text{cut}}) + \Gamma(c\bar{b}_8(^3S_1), x_l^{\text{cut}})} \quad (41)$$

for the S -wave color-octet component $|c\bar{b}_8(^3S_1)\rangle$, and

$$R_P = \frac{\Gamma(c\bar{b}_1(^1S_0), x_l^{\text{cut}})}{\Gamma(c\bar{b}_1(^1S_0), x_l^{\text{cut}}) + \Gamma(c\bar{b}_8(^1P_1), x_l^{\text{cut}})}, \quad (42)$$

for P -wave color-octet state $|c\bar{b}_8(^1P_1)\rangle$, which depend on the cut of the lepton energy x_l^{cut} . Here

TABLE I. The ratios of the integrated partial width R_S and R_P for case (A) ($\Delta_S=0.1, \Delta_P=0.1$) and case (B) ($\Delta_S=0.3, \Delta_P=0.3$). (The definition of R_S , R_P , Δ_S , Δ_P , and x_l^{cut} is given in text.)

	Case (A) ($\Delta_S=0.1$)				Case (B) ($\Delta_S=0.3$)			
x_l^{cut}	0.80	0.85	0.90	0.95	0.80	0.85	0.90	0.95
R_S	0.257	0.191	0.122	0.047	0.037	0.026	0.015	0.005
	Case (A) ($\Delta_P=0.1$)				Case (B) ($\Delta_P=0.3$)			
x_l^{cut}	0.90	0.92	0.94	0.96	0.80	0.85	0.90	0.95
R_P	0.280	0.212	0.154	0.089	0.132	0.081	0.041	0.014

$$\Gamma(c\bar{b}_1(^1S_0), x_l^{\text{cut}}) \equiv \int_{x_l^{\text{cut}}}^{1-\delta} dx \frac{d\Gamma(c\bar{b}_1(^1S_0))}{dx}, \quad (43)$$

$$\Gamma(c\bar{b}_8(^3S_1), x_l^{\text{cut}}) \equiv \int_{x_l^{\text{cut}}}^{1-\delta} dx \frac{d\Gamma(c\bar{b}_8(^3S_1))}{dx}, \quad (44)$$

and

$$\Gamma(c\bar{b}_8(^1P_1), x_l^{\text{cut}}) \equiv \int_{x_l^{\text{cut}}}^{1-\delta} dx \frac{d\Gamma(c\bar{b}_8(^1P_1))}{dx}, \quad (45)$$

with $\delta = m_g/M$ and a giving tiny gluon mass $m_g = 0.2$ GeV (the cut δ at $x_l \approx 1$ is necessary for the OPE expansion to be available in PQCD calculations and to dictate the experimental capacity in the energy resolution on the charged lepton, etc.). We evaluate them and put the results in Table I.

From Fig. 6 and Table I, one may see that there is a possibility to verify the color-octet components in the meson B_c , which may play visible roles in the B_c annihilation $B_c \rightarrow l^+ \nu_l + \text{hadrons}$ experimentally. Although NRQCD is a very absorbing theory, it still needs to be widely verified; thus we think that our estimates should address experimentalists' attention. In conclusion, further study of the possibility to verify color octet components in the meson B_c more quantitatively is indicated. Monte Carlo simulations for the B_c meson in hadronic collision environments are in progress [22].

ACKNOWLEDGMENTS

The authors would like to thank Professor J.-P. Ma for useful discussions. This work was supported in part by the National Natural Science Foundation of China (NSFC).

APPENDIX: INTEGRATION FORMULA OF THE B_c COLOR-SINGLET MESON

A number of kinematic variables appear repeatedly in the paper. For convenience, all of them are collected here. P , k_1 , k_2 , k_4 , k_5 denote the four-momenta of the particles, and the auxiliary momenta, $Q=k_1+k_2$ and $k=k_4+k_5$, characterize the gluon-gluon system and the virtual W (lepton pair), respectively.

The scaled masses and lepton energies

$$y = \frac{k^2}{M^2}, \quad z = \frac{Q^2}{M^2}, \quad x_l = \frac{2E_l}{M}, \quad x_\nu = \frac{2E_\nu}{M} \quad (\text{A1})$$

vary in the region

$$\begin{aligned} 0 &\leq x_l \leq 1, \\ 0 &\leq y \leq x_l, \\ 0 &\leq z \leq z_{\max} = (1-x_l) \left(1 - \frac{y}{x_l}\right), \end{aligned} \quad (\text{A2})$$

where the lepton masses are ignored. Frequently used kinematical variables that characterize the gluon-gluon system are

$$\begin{aligned} R_0 &= \frac{(1-y+z)}{2}, \\ R_3 &= \frac{\sqrt{(1-y+z)^2 - 4z}}{2}, \\ Y_P &= \ln \left(\frac{(R_0 + R_3)^2}{z} \right). \end{aligned} \quad (\text{A3})$$

All of the variables are scaled by B_c -meson mass so as to make them dimensionless in the coefficients c_i .

To calculate the annihilation, one observes that the squared matrix element can be ‘‘factorized’’ into the leptonic tensor $L_{\mu\nu}(k_4, k_5)$ and the hadronic tensor $T_{\mu\nu}(P, k_1, k_2) \equiv A_\mu^* \cdot A_\nu$, (A_μ is the amplitude). To perform integration over the gluon-gluon phase space, the resultant integration $t_{\mu\nu}$ depends on P and $Q=k_1+k_2$ only:

$$\begin{aligned} t_{\mu\nu}(P, Q) &= \int dR_2(Q; k_1, k_2) T_{\mu\nu}(P, k_1, k_2), \\ &= d_{1,\mu\nu}(^1S_0; P, k) \frac{1}{M^2} \langle B_c | \psi_c^\dagger \chi_b \chi_b^\dagger \psi_c | B_c \rangle, \end{aligned} \quad (\text{A4})$$

where dR_2 is defined by

$$\begin{aligned} dR_2(Q; k_1, k_2) &= (2\pi)^4 \delta(Q - k_1 - k_2) \\ &\times \frac{d^3\vec{k}_1}{2(2\pi)^3 E_1} \frac{d^3\vec{k}_2}{2(2\pi)^3 E_2}, \end{aligned} \quad (\text{A5})$$

and the tensor $d_{1,\mu\nu}(^1S_0; P, k)$ has the general structure

$$\begin{aligned} d_{1,\mu\nu}(^1S_0; P, k) &= A g_{\mu\nu} + B P_\mu P_\nu + C Q_\mu Q_\nu \\ &+ D P_\mu Q_\nu + E Q_\mu P_\nu. \end{aligned} \quad (\text{A6})$$

For the massless lepton pair, the lepton current is conserved, $k_\mu L^{\mu\nu} = k_\nu L^{\mu\nu} = 0$, where $k = P - Q$ is the total momentum of the lepton pair. With this equation, Eq. (A6) can be further simplified as

$$\begin{aligned} d_{1,\mu\nu}(^1S_0; P, k) &= A g_{\mu\nu} + (B + C + D + E) P_\mu P_\nu \\ &= A g_{\mu\nu} + B' P_\mu P_\nu. \end{aligned} \quad (\text{A7})$$

Instead of integrating the tensor $T_{\mu\nu}$, it is sufficient to integrate the following scalar projections:

$$\begin{aligned} c_1 &= \frac{M^2}{\langle B_c | \psi_c^\dagger \chi_b \chi_b^\dagger \psi_c | B_c \rangle} \int dR_2 T_{\mu\nu} P^2 g^{\mu\nu}, \\ c_2 &= \frac{M^2}{\langle B_c | \psi_c^\dagger \chi_b \chi_b^\dagger \psi_c | B_c \rangle} \int dR_2 T_{\mu\nu} P^\mu P^\nu, \end{aligned} \quad (\text{A8})$$

and the coefficients A , B' , . . . can be expressed in terms of the scalar functions c_i , $i=1,2$ as follows:

$$A = \frac{c_1 - c_2}{3P^2}, \quad B' = \frac{4c_2 - c_1}{3P^4}. \quad (\text{A9})$$

The numerators of c_i are given by polynomials in (Pk_1) and (Pk_2) with coefficients depending on y , z , $(QP) = M^2 R_0$, and $(Qk_1) = (Qk_2) = M^2 z/2$. In fact, all of the phase space integrations may be attributed to the following integrations:

$$I_{m,n} = \int dR_2(Q; k_1, k_2) (Pk_1)^m (Pk_2)^n \quad (-2 \leq m, n \leq 0). \quad (\text{A10})$$

Because of the Lorentz invariance, we evaluate the integral in the $Q=k_1+k_2$ rest system and the results show

$$\begin{aligned} I_{0,0} &= \frac{1}{8\pi}, \\ I_{-1,0} = I_{0,-1} &= \frac{Y_P}{8\pi M^2 R_3}, \\ I_{-2,0} = I_{0,-2} &= \frac{1}{2\pi M^4 z}, \\ I_{-2,-1} = I_{-1,-2} &= \frac{1}{4\pi M^6} \left(\frac{Y_P}{R_3 R_0^2} + \frac{2}{z R_0} \right), \\ I_{-1,-1} &= \frac{Y_P}{4\pi M^4 R_0 R_3}, \\ I_{-2,-2} &= \frac{1}{4\pi M^8} \left(\frac{Y_P}{R_3 R_0^3} + \frac{2}{z R_0^2} \right). \end{aligned} \quad (\text{A11})$$

The explicit form of c_i is shown in the following, where a common factor $(2\pi/3)\alpha_s^2$ is contracted out for convenience and the terms that can be obtained by interchanging m_b and m_c are not shown explicitly, that is, the actual value of each c_i equals $c_i + c_i(r_1 \leftrightarrow r_2)$, where $r_1 = m_b/M$ and $r_2 = m_c/M$:

$$\begin{aligned}
c_1 = & \frac{16}{f_1^2 f_2 z r_1^2 r_2^2 R_0^2} (-8r_1^3 r_2 [3f_2 z + 4(f_2 - f_1)r_2^2] R_0^2 + f_1^2 f_2 (y z + 4R_0^2) - 4f_1 r_1 r_2 [f_1 f_2 z + 2f_2(f_1 - z)R_0 \\
& + (2f_1 f_2 + z - 4f_2 z + 4f_2 r_2) R_0^2] + 8r_1^2 \{f_2 z (-f_1 + z) R_0^2 + f_2 r_2 R_0^2 [3z + (4f_1 - 2z)R_0] - 4f_2 r_2^3 R_0 (2f_1 + R_0 + R_0^2) \\
& + r_2^2 [2f_1^2 f_2 + R_0^2 (4f_2 - 4f_1 f_2 + 5f_1 z - 2f_1 R_0 + 4f_2 R_0^2)]\}) + \frac{8Y_P}{f_1^2 f_2 z r_1^2 r_2^2 R_0^3 R_3} [16f_2 z r_1^4 R_0^2 + f_1^2 f_2 z (y - 2R_0^2) \\
& + 4f_1 r_1 \{-(f_1 f_2 z r_2) - 2f_2 (f_1 - z) r_2 R_0 + r_2 [2f_1 f_2 + z(z - 1 - 2f_2) + 4f_2 (3 - 2r_2) r_2] R_0^2 + 2(f_2 z - 2z r_2 + 2f_2 r_2^2) R_0^3 \\
& + 4r_2 R_0^4\} + 8r_1^3 r_2 R_0^2 [3f_2 z + 4r_2 (f_1 r_2 + f_2 R_0)] + 8r_1^2 (-2f_2 z R_0^2 + 4f_2 r_2^4 R_0^2 + f_2 (-2f_1 + z) R_0^4 - 4f_2 r_2^3 R_0 (2f_1 + R_0^2) \\
& + f_2 r_2 R_0^2 [z - 2R_0 (2 - 2f_1 + z + 2R_0^2)] + r_2^2 \{2f_1^2 f_2 + R_0^2 [-4f_1 f_2 + 4f_1 z + 3f_2 z - 4(f_1 - f_2) R_0 (1 + R_0)]\}), \quad (A12)
\end{aligned}$$

$$\begin{aligned}
c_2 = & \frac{8}{f_1^2 f_2 z r_1^2 r_2^2 R_0^2} \{f_1^2 f_2 [z^2 + 8r_1 r_2 (-z + 4r_1 r_2)] - 4f_1 f_2 r_1 R_0 \{r_2 (4f_1 - z R_0) + r_1 [z R_0 + 16r_2^2 (-2r_2 + R_0)]\} \\
& + 2R_0^2 [f_1^2 f_2 z + 2r_1 (f_1 f_2 z - 2f_1 r_2 (z + 3f_2 z + 4f_2 r_2) - 4r_1^2 r_2^2 [f_2 + 2(-f_1 + f_2) r_2 - 2f_2 R_0] + r_1 \{f_2 z^2 + 2r_2^2 [5f_1 z \\
& + 2f_2 (y + z) + 2f_2 r_2 (1 + 2r_2 - 2R_0) - 4f_1 R_0\}]\}) + \frac{8Y_P}{f_1^2 f_2 z r_1^2 r_2^2 R_0^3 R_3} \{f_1^2 f_2 z^2 + 8f_1^2 f_2 r_1 r_2 (-z + 4r_1 r_2) \\
& - 16f_1 f_2 r_1 r_2 (f_1 - 8r_1 r_2^2) R_0 + 2[f_1^2 f_2 (1 - 2z) + 2r_1 (f_2 z [f_1 + (-2 - 3f_1 + 4y) r_1] + f_1 [4f_1 f_2 + (-3 + f_2 + y) z] r_2 \\
& - 4\{2f_1 f_2 + r_1 [8f_1 f_2 - (3f_1 + f_2) z + 2f_1 (-1 + r_1) r_1\}] r_2^2 + 8f_1 r_1^2 r_2^3 + 16f_2 r_1 r_2^4\} R_0^2 \\
& - 16r_1 (-[f_1 r_2 (1 + f_2 - y + 2f_2 r_2)] - r_1^2 \{f_2 z + r_2 [f_2 - (f_1 - 2f_2) r_2]\}) + r_1 r_2 \{f_2 (-4f_1 + y + z) \\
& + r_2 [2f_1 + f_2 + (f_1 + 6f_2) r_2]\} R_0^3 - 16r_1^2 r_2 [2f_2 r_1 + (f_1 - 3f_2) r_2] R_0^4\}, \quad (A13)
\end{aligned}$$

where $f_1 = -1 + y + 2r_1 R_0$, $f_2 = -1 + y + 2r_2 R_0$.

After contraction of the hadronic tensor with the leptonic tensor $L_{\mu\nu}(k_4, k_5)$, replacing Q by $P - k$, and substituting

$$(k_4 k_5) = \frac{M^2 y}{2}, \quad (k k_4) = (k k_5) = \frac{M^2 y}{2}, \quad (P k_4) = \frac{M^2 x_l}{2}, \quad (A14)$$

$$(P k_5) = \frac{M^2 x_\nu}{2}, \quad (P k) = \frac{M^2 (1 + y - z)}{2},$$

$$x_\nu = 1 + y - z - x_l. \quad (A15)$$

The task now left is to integrate the integrand of x_l , y , and z , and it can be completed numerically.

-
- [1] CDF Collaboration, F. Abe *et al.*, Phys. Rev. D **58**, 112004 (1998).
- [2] Chao-Hsi Chang and Yu-Qi Chen, Phys. Rev. D **46**, 3845 (1992); **50**, 6013(E) (1994); **48**, 4086 (1993); Chao-Hsi Chang, Yu-Qi Chen, Guo-Ping Han, and Hung-Tao Jiang, Phys. Lett. B **364**, 78 (1995); Chao-Hsi Chang, Yu-Qi Chen, and R. J. Oakes, Phys. Rev. D **54**, 4344 (1996); E. Braaten, K. Cheung, and T. C. Yuan, *ibid.* **48**, 4230 (1993); **48**, R5049 (1993); A. V. Berezhnoy, V. V. Kiselev, A. K. Likhoded, and A. I. Onishchenko, Yad. Fiz. **60**, 1866 (1997); K. Kolodziej, A. Leike, and R. Rückl, Phys. Lett. B **355**, 337 (1995).
- [3] Chao-Hsi Chang and Yu-Qi Chen, Phys. Rev. D **49**, 3399 (1994); Commun. Theor. Phys. **23**, 451 (1995).
- [4] Chao-Hsi Chang, Yu-Qi Chen, Guo-Li Wang, and Hong-Shi Zong, Phys. Rev. D **65**, 014017 (2002); Commun. Theor. Phys. **35**, 395 (2001).
- [5] M. Lusignoli and M. Masetti, Z. Phys. C **51**, 549 (1991); N. Isgur, D. Scora, B. Grinstein, and M. Wise, Phys. Rev. D **39**, 799 (1989); D. Scora and N. Isgur, *ibid.* **52**, 2783 (1995); D.-S. Du, G.-R. Lu, and Y.-D. Yang, Phys. Lett. B **387**, 187 (1996); Dongsheng Du *et al.*, *ibid.* **414**, 130 (1997); A. Abd El-Hady, J. H. Munoz, and J. P. Vary, Phys. Rev. D **62**, 014019 (2000); P. Colangelo and F. De Fazio, *ibid.* **61**, 034012 (2000); V. V. Kiselev, A. E. Kovalsky, and A. K. Likhoded, Nucl. Phys. **B585**, 353 (2000); M. A. Nobes and R. M. Woloshyn, J. Phys. G **26**, 1079 (2000).
- [6] M. Beneke and G. Buchalla, Phys. Rev. D **53**, 4991 (1996).
- [7] Chao-Hsi Chang, Shao-Long Chen, Tai-Fu Feng, and Xue-

- Qian Li, Phys. Rev. D **64**, 014003 (2001); Commun. Theor. Phys. **35**, 51 (2001).
- [8] Chao-Hsi Chang, Jian-Ping Cheng, and Cai-Dian Lü, Phys. Lett. B **425**, 166 (1998).
- [9] Chao-Hsi Chang, Cai-Dian Lü, Guo-Li Wang, and Hong-Shi Zong, Phys. Rev. D **60**, 114013 (1999).
- [10] Chao-Hsi Chang, Anjan K. Giri, Rukmani Mohanta, and Guo-Li Wang, J. Phys. G **28**, 1403 (2002).
- [11] M. Kobayashi, T.-T. Lin, and Y. Okada, Prog. Theor. Phys. **95**, 361 (1996); C. H. Chen, C. Q. Geng, and C. C. Lih, Phys. Rev. D **56**, 6856 (1997); G.-H. Wu and J. N. Ng, *ibid.* **55**, 2806 (1997); C. Q. Geng and S. K. Lee, *ibid.* **51**, 99 (1995).
- [12] T. M. Aliev and M. Savci, Phys. Lett. B **434**, 358 (1998); J. Phys. G **25**, 1205 (1999).
- [13] J. P. Ma and J. S. Xu, Eur. Phys. J. C **24**, 261 (2002).
- [14] G. T. Bodwin, E. Braaten, and G. P. Lepage, Phys. Rev. D **51**, 1125 (1995); **55**, 5853(E) (1997).
- [15] Yu-Qi Chen and Yu-Ping Kuang, Phys. Rev. D **46**, 1165 (1992); E. Eichten and C. Quigg, *ibid.* **49**, 5845 (1994); A. Abd El-Hady, J. H. Munoz, and J. P. Vary, *ibid.* **55**, 6780 (1997).
- [16] E. Braaten and Yu-Qi Chen, Phys. Rev. D **55**, 2693 (1997).
- [17] S. Mandelstam, Proc. R. Soc. London **233**, 248 (1955).
- [18] J. L. Cortes, X. Y. Pham, and A. Tounsi, Phys. Rev. D **25**, 188 (1982).
- [19] A. Pineda and F. J. Yudurain, Phys. Rev. D **58**, 094022 (1998).
- [20] F. J. Yudurain, hep-ph/0002237.
- [21] N. Brambilla, D. Eiras, A. Pineda, J. Soto, and A. Vairo, Phys. Rev. D **67**, 034018 (2003).
- [22] Xing-Gang Wu *et al.*, B_c Monte Carlo generator and relevant simulations are in progress.